

## Electron Temperature Scaling in Laser Interaction with Solids

T. Kluge,\* T. Cowan, A. Debus, U. Schramm, K. Zeil, and M. Bussmann

*Helmholtz-Zentrum Dresden-Rossendorf e.V., Bautzner Landstraße 400, D-01328 Dresden, Germany*

(Received 27 July 2011; published 10 November 2011)

A precise knowledge of the temperature and number of hot electrons generated in the interaction of short-pulse high-intensity lasers with solids is crucial for harnessing the energy of a laser pulse in applications such as laser-driven ion acceleration or fast ignition. Nevertheless, present scaling laws tend to overestimate the hot electron temperature when compared to experiment and simulations. We present a novel approach that is based on a weighted average of the kinetic energy of an ensemble of electrons. We find that the scaling of electron energy with laser intensity can be derived from a general Lorentz invariant electron distribution ansatz that does not rely on a specific model of energy absorption. The scaling derived is in perfect agreement with simulation results and clearly follows the trend seen in recent experiments, especially at high laser intensities where other scalings fail to describe the simulations accurately.

DOI: 10.1103/PhysRevLett.107.205003

PACS numbers: 52.38.Kd, 52.30.-q, 52.38.Dx, 52.65.Rr

One of the most important and yet controversial physics issues in short-pulse laser-solid interaction is the determination of the temperature and number of hot electrons accelerated by the intense fields of the laser pulse [1–4]. Many applications—including fast ignition schemes, femtosecond diffractometry, ion acceleration, and x-ray production—depend crucially on achieving the highest possible conversion efficiency and electron temperature with the minimum amount of laser energy possible [4]. Thus, deducing the scaling of hot electron temperature from laser intensity is of great importance, yet, up until now there exists no consistent analytical model that can accurately predict the scalings seen in experiments and simulations for both nonrelativistic *and* relativistic intensities. This is partly due to the fact that depending on preplasma scale length, intensity and polarization of the laser pulse, the absorption of laser energy by electrons can be described by various processes like resonance absorption [5], skin layer heating [6], Brunel heating [7], and  $v \times B$  heating [8]. The scaling introduced in this letter overcomes the need for a specific absorption model by introducing a Lorentzian scalar steady state distribution function for the electron energy. This distribution function is then used to derive a general expression for the electron mean energy. Finally, we identify this mean energy with the hot electron temperature and derive its scaling with laser intensity from the simple electron quiver motion in the electromagnetic wave. (We adopt the term “temperature” as a synonym for the average kinetic energy in order to compare our results with previous publications and experiments. This term is commonly used in laser-matter interaction theory due to the existence of a quasiexponential slope found in the energy spectrum of hot electrons both in experiments and simulations [9]. It does not strictly resemble a temperature in the thermodynamics sense, since during the laser plasma interaction the situation is nonequilibrium, and it would imply a vanishing mean electron flow velocity.) In a plane traveling

electromagnetic wave with angular frequency  $\omega_0$  and wave vector  $\mathbf{k}_0 = k_0 \mathbf{e}_z$  the fields are given by  $\mathbf{a} = \mathbf{E}/E_0 = e\mathbf{E}/(m_e c \omega_0) = a_0 \cos(\omega_0 t - k_0 z) \mathbf{e}_x$  and  $\mathbf{b} = \mathbf{B}/B_0 = e\mathbf{B}/(m_e \omega_0) = -a_0 \cos(\omega_0 t - k_0 z) \mathbf{e}_y$  and the transverse canonical momentum is conserved [10]. Using Lorentz’s equation one then finds for single electrons initially at rest that the momenta  $p_x(t)$ ,  $p_z(t)$  and energy  $\gamma(t) = \sqrt{1 + \mathbf{p}^2}$  are given by [4]

$$p_x(t) = a_0 \sin[\omega_0 t - k_0 z(t)], \quad (1)$$

$$\gamma(t) - p_z(t) = 1, \quad (2)$$

and, hence  $p_z(t) = p_x(t)^2/2$ , assuming an adiabatic laser ramp-up. Note that here and throughout the Letter a unit system where the speed of light, electron mass, electron charge are unity,  $c = m_e = e = 1$ . As a measure for the laser intensity  $I$  we introduce the laser strength parameter  $a_0 = [2I/(n_c m_e c^3)]^{1/2}$  where  $n_c = m_e \epsilon_0 \omega_0^2 e^{-2}$  is the critical density of the cold plasma.

When a relativistic plane wave interacts with an ensemble of electrons initially at rest, the electrons will be randomly injected into the wave’s phase. The average kinetic energy at any time, averaged over all hot electrons, is given by  $\langle \gamma \rangle = \frac{\int \gamma f_\gamma d\gamma}{\int f_\gamma d\gamma}$ , where  $f_\gamma = dN/d\gamma$  is the energy distribution function of the electrons. With the laser wave propagating at velocity  $c\mathbf{e}_z$ ,  $\mathbf{a}(\varphi)$  is a periodic function with period  $2\pi$  in  $\varphi = \omega_0 t - k_0 z$ . If we neglect effects such as repeated heating [11,12], the electron energy must be a periodic function with the same period as  $\mathbf{a}(\varphi)$  and the average can then be written as

$$\langle \gamma \rangle = \frac{\int_0^{t(\varphi=2\pi)} \gamma(t) f_t dt}{\int_0^{t(\varphi=2\pi)} f_t dt}. \quad (3)$$

Since the electron distribution  $f_t = dN/dt$  is difficult to derive *ab initio*, we derive  $f_\varphi = dN/d\varphi$  and then use

$f_t = dN/d\varphi d\varphi/dt$ . This approach has the advantage that  $f_\varphi$  transforms as a scalar under Lorentz transformation, and thus remains constant throughout the interaction with the laser. For this to be valid, one only has to assume (2) to be fulfilled without any further assumption on the laser field, especially one may drop the plane wave assumption. In that case, the phase shift of an electron is proportional to its proper time,  $d\varphi = (1 - \beta_z)dt = \gamma^{-1}dt = d\tau$ . Assuming a uniform electron distribution at  $t_0 = \tau_0 = 0$  before the laser pulse has been switched on, the distribution  $dN/d\varphi$  will remain uniform for a given electron proper time  $\tau_1 > 0$ ,  $dN/d\varphi|_{\tau=\tau_1} = \text{const}$  [see Fig. 2(a)]. The requirement  $\tau = \tau_1$  for all electrons is equivalent to the adiabatic ramp-up condition used before, because then the electron motion in the laser wave does not depend on its initial phase  $\varphi_i(\tau_0)$ .

In order to exemplify this we consider the case of a plane wave and free electrons in vacuum. Using the conservation of the 4-momentum of the combined system of particles and fields [10] we again determine  $f_\varphi = dN/d\varphi$ . Considering the conservation of energy transferred from the laser to electrons during one cycle in a steady state and assuming a phase independent absorption fraction  $\eta$ , the field energy absorbed in a given volume equals the sum over the kinetic energy acquired by all particles therein. Hence at a fixed time in the laboratory frame we find with  $dz = -d\varphi$

$$\begin{aligned} \eta \int_0^{2\pi} a_0^2 \cos^2(t - z) dz &= \int_0^{2\pi} \sum_{i=1}^N [(\gamma_i - 1) \delta(z - z_i)] dz \\ &= \int_0^{2\pi} \sum_{i=1}^{dN} [(\gamma_i - 1) \delta(\varphi - \varphi_i)] d\varphi \\ &= \int_0^{2\pi} (\bar{\gamma}(\varphi) - 1) f_\varphi d\varphi, \end{aligned}$$

where  $\bar{\gamma}(\varphi) = \int_\varphi^{\varphi+d\varphi} \sum_{i=1}^{dN} [\gamma_i \delta(\varphi - \varphi_i)] d\varphi / \Delta N$  is the average electron energy of the  $\Delta N$  electrons with  $\varphi_i \in [\varphi, \varphi + d\varphi]$ . Assuming the laser intensity has been ramped up adiabatically, from (1) and (2) we have  $\gamma - 1 = a_0^2 \sin^2 \varphi / 2$  for a free electron in a plane wave. Setting the average electron kinetic energy  $\bar{\gamma}(\varphi) - 1$  equal to the single electron adiabatic energy, it follows the trivial solution  $f_\varphi = \text{const}$ .

Instead of assuming a uniform electron distribution in the laboratory time [as implicitly done in [13]; see Eq. (8)] or postulating *ad hoc*  $n_{\text{hot}} = \gamma n_c$  (as done in [3]), we find the electrons to be distributed uniformly with respect to the retarded wave coordinate  $\varphi$ , which is equal to the electron proper time. Hence,  $f_t$  is given by

$$f_t = \frac{dN}{d\varphi} \frac{d\varphi}{dt} \propto \frac{1}{\gamma}. \quad (4)$$

Now substituting (4) into (3) one finally obtains the result

$$\langle \gamma \rangle = \frac{2\pi}{\int_0^{2\pi} \frac{1}{\gamma} dt}. \quad (5)$$

This important relation states that the average kinetic energy of the accelerated electrons is equal to the inverse of the unweighted average of the inverse of the single electron energy  $\gamma(t)$  with respect to laboratory time  $t$ . In other words, the average electron kinetic energy is obtained by averaging the single electron energy with respect to the phase  $\varphi$  or to the electron proper time. Consequently, the average energy of an electron ensemble cannot be derived simply by averaging the single electron energy over the laboratory time.

The key to inferring the hot electron temperature from a given laser intensity now lies in deducing  $\langle \gamma \rangle$  from the electron dynamics at the critical surface. For this we focus on the important case of laser normal incidence. At oblique laser incidence most additional heating mechanisms are suppressed in the presence of a density gradient and/or high laser intensities (see [7] within limits) and the electron temperature approaches that of normal incidence.

In the following we will first consider the case of a steplike density gradient and high electron density  $n_e \gg 1$  and then discuss the more realistic case of a preplasma with the existence of a region of  $n_e \approx 1$ .

At a steep density interface the plasma can build up an electric field that tends to balance the ponderomotive force at any time [14], the electron motion is then governed in first order by the quiver motion parallel to the plasma interface only (almost transverse solution [15]),

$$\gamma_x(t) = \sqrt{1 + p_x^2(t)} \quad (6)$$

Using Eq. (1), the unweighted average over *laboratory time* thus reads  $\langle \gamma_x \rangle_t = \int_0^{2\pi} \sqrt{1 + a_0^2 \sin^2(\omega_0 t)} dt / 2\pi$  and hence the temperature would be given by

$$T_{\text{hot,osc}} = \frac{2E(-a_0^2)}{\pi} - 1, \quad (7)$$

where  $E(-a_0^2)$  is the complete elliptical integral of the second kind. For  $a_0 \ll 1$  this expression converges with the ponderomotive scaling [16]

$$T_{\text{hot,pond}} = \gamma_{\text{pond}} - 1 = \sqrt{1 + \frac{a_0^2}{2}} - 1, \quad (8)$$

which to describe the electron temperature at a flat solid has been first suggested by Wilks *et al.* [13]. For  $a_0 \gg 1$  Eq. (7) gives only small correction to (8), by a factor of less than  $2^{3/2}/\pi$ , and cannot explain the low temperatures observed experimentally and numerically for large  $a_0$ . Experiments [17–20] at intensities ranging from  $a_0 \approx 0.2$  to 20 attempting to measure the electron temperature show a large scatter in their results but seem to suggest the average total electron kinetic energy to be considerably below the ponderomotive energy (see Fig. 1). E.g., a recent

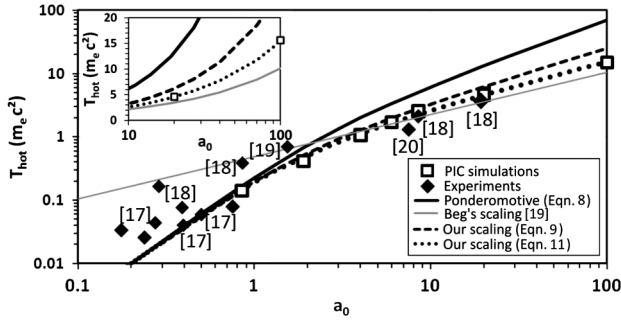


FIG. 1. Comparison of various temperature scalings with selected experimental values (diamonds) and PIC simulations (squares). Simulations include ionizations and collisions, target is a flat foil with thickness  $5\lambda$  of copper ions, covered with a  $2\lambda$  thick proton layer. The pulse duration of the Gaussian pulse with waist  $2\lambda$  (a test simulation with a plane wave at  $a_0 = 100$  yields a similar temperature) was fixed at  $100\omega_0^{-1}$ . To reduce computational demands, the electron density when fully ionized was set to  $10n_c$ ,  $40n_c$  or  $100n_c$  for intensities with  $a_0 < 8.5$ ,  $8.5 \leq a_0 \leq 20$  or  $a_0 = 100$ . This choice results in a skin-length  $\delta \geq \lambda/2$ , a situation corresponding to a realistic solid density case with sufficient preplasma at the front surface.

experiment [18] found a temperature of about  $2 \times 0.511$  MeV for  $a_0 \approx 8.5$  which is significantly below the ponderomotive temperature of  $5.1 m_e c^2$ . This fact had been expressed already by Beg [19] in the empirical scaling  $T_{\text{hot,Beg}} \approx 0.469 a_0^{2/3}$ . While for small  $a_0$  the average total kinetic electron energy scaling seen in our 2D3V particle-in-cell (PIC) simulations using the code IPICLS [21] coincides with (8) we find it to be significantly below the ponderomotive energy for  $a_0 \gg 1$  (Fig. 1), in agreement with the experiments, yet higher than predicted by the Beg scaling. In [3] an attempt was made to explain the weaker electron temperature scaling, but it does not fit our simulations for high intensities  $a_0 \gg 1$  nor does it converge with the ponderomotive scaling for small intensities  $a_0 \ll 1$  as one would expect from a fully consistent theory.

Following our model, the average energy of an electron ensemble cannot be derived simply by averaging the single electron energy over the laboratory time, so (7) does generally not give  $\langle \gamma \rangle$ . Only for nonrelativistic intensities and hence small  $|\beta| \ll 1$  the unweighted time averaged energy  $\langle \gamma \rangle_t$  converges with the average energy given by (5). Averaging Eq. (6) according to our result Eqn. (5), we find the temperature scaling  $T_e^{\text{hot}} = 2\pi [\int_0^{2\pi} (1 + a_0^2 \sin^2 \omega_0 t)^{-1/2} dt]^{-1} - 1$  which is significantly less than Eqs. (7) and (8) for  $a_0 \gg 1$ . It can be expressed using the complete elliptical integral of the first kind,  $K(-a_0^2)$ , by

$$T_e^{\text{hot}} + 1 = \frac{\pi}{2K(-a_0^2)}. \quad (9)$$

Simple analytic expressions for  $T_e^{\text{hot}}$  can be given for the extreme cases  $a_0 \ll 1$  and  $a_0 \gg 1$ ,

$$T_e^{\text{hot}} + 1 = 1 + \frac{a_0^2}{4} + O(a_0^4) \quad (a_0 \ll 1),$$

$$T_e^{\text{hot}} + 1 = \frac{\pi a_0}{2 \ln 16 + 2 \ln a_0} + O(a_0^{-3}) \quad (a_0 \gg 1),$$

We now analyze the more realistic case including a certain amount of preplasma to be present in front of the foil, e.g., due to laser prepulses or ASE, which will give some correction to (9). The laser field can penetrate the foil up to a skin depth  $\delta > \lambda/2$  as an evanescent wave and the electron motion no longer is limited to the foil surface. Electric and magnetic fields decrease exponentially with increasing depth and the magnetic field changes its sign at the interface. To estimate the resulting temporal field evolution seen by a hot electron, we consider the fields observed by a virtual test particle moving forward with  $c$  in dependence of the phase of the wave when it crosses the plasma boundary at  $z = 0$ . Two limits are observed [Figs. 2(c) and 2(d)]. One is given by  $a \approx 2a_0 \cos(\omega_0 t)$ ,  $b \approx 0$ , where  $t \equiv 0$  is the time when  $z = 0$ . In this limit an electron starting at  $z = 0$  will experience no longitudinal forces due to the vanishing magnetic field, so there is no net transfer of energy to the plasma. In the other limit it is  $E/E_0 = -B/B_0 = a(t) = \cos(\omega_0 t)$ . In that limit an electron will experience a large longitudinal field and can thus detach from the surface, keeping its energy and being absorbed into the foil. The result are bunches emitted into and traveling through the foil at a frequency of  $2\omega_0$  and a separation of  $\lambda/2$  [Fig. 2(b)]. It can easily be shown that (2) is still true, so the electron distribution is still given by (4) and we can assume (5) to be still valid. With the

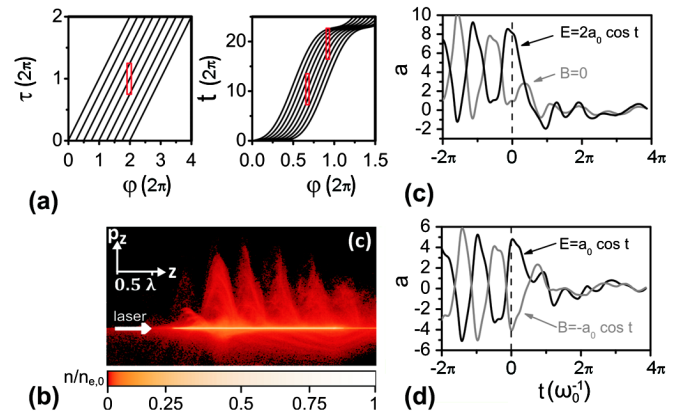


FIG. 2 (color online). (a) Trajectories of electrons distributed uniformly at  $t_0 = \tau_0 = 0$ , assuming adiabatic ramp up of laser intensity ( $a_0 = 5$ ).  $f_\tau$  is constant while  $f_t = \gamma^{-1}$ , as indicated by trajectories crossing the red boxes. (b) Electron phase space density in the  $z - p_z$  plane at the time the laser maximum reaches the foil front surface. Electrons are emitted into the target in bunches separated by  $\lambda/2$ . Parameters are the same as in Fig. 1 with  $a_0 = 5$ . (c),(d) Limiting cases for the temporal evolution of fields at the position of a virtual particle moving forward with  $c$ , crossing the critical density surface at  $t = 0$ .

above fields and with (1), (2), the Lorentz equation for the transverse momentum component reads

$$\frac{dp_x}{dt} = a(t) + v_z b(t) = a_0 \left( 1 - \frac{p_x^2}{2 + p_x^2} \right) \cos \omega_0 t. \quad (10)$$

This equation resembles a Riccati differential equation and can be solved analytically. The result reads

$$p_x(t) = S - \frac{2}{S},$$

$$S = \sqrt[3]{\sqrt{(3a_0 \sin \omega_0 t)^2 + 8} + 3a_0 \sin \omega_0 t}. \quad (11)$$

It is now straightforward to obtain the single electron temporal energy evolution  $\gamma(t)$  using (1) and (2). Averaging the inverse  $\gamma(t)^{-1}$  over time and taking its inverse according to (5), we finally obtain a prediction for the electron temperature, shown in Fig. 1 by the dotted line [in the following referred to as scaling (11)] and contrasted with the ponderomotive scaling (8) (solid line). Scaling (11) is in remarkable agreement with the PIC results up to the highest simulated intensity with  $a_0 = 100$  where the ponderomotive scaling significantly overestimates the electron temperature. The deviation between our model and PIC is less than 5% for all  $a_0$ , while, for example, the scaling presented in [3] for  $a_0 = 100$  is off by more than 30% and the ponderomotive scaling is off by even almost an order of magnitude. Unlike the scaling from [3], our model converges with the ponderomotive scaling for  $a_0 \leq 1$  as expected. Compared to (9), scaling (11) yields moderately lower temperature values since we assumed the transverse canonical momentum to be conserved, which is not true for the fields assumed in the critical density region [Fig. 2(d)].

Finally, we illustrate the importance of the above by the example of the maximum energy  $\epsilon_{\max}$  of ions accelerated following the laser-electron interaction. The longer the pulse duration, the more does the temperature influence

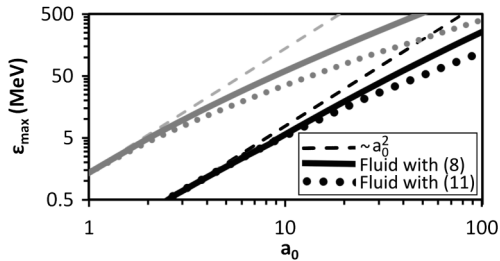


FIG. 3. Comparison of proton maximum energy as a function of  $a_0$  for ponderomotive electron temperature scaling (8) (solid) and our scaling (11) (dotted). Parameters are the same as for PIC simulations (Fig. 2), assuming a laser absorption of 25% and electron divergence of  $40^\circ$  based on the simulations. Pulse duration  $\tau = 100\omega_0^{-1}$  (black) and  $\tau = 1000\omega_0^{-1}$  (gray), demonstrating the stronger effect of the temperature scaling for long pulses. Dashed lines indicate  $\epsilon_{\max} \propto a_0^2$ .

$\epsilon_{\max}$  and the more important becomes the correct modeling of the electron temperature scaling (Fig. 3). This can be seen, for example, from a time limited fluid model used for target normal sheath acceleration of protons [11,22,23],  $\epsilon_{\max} \approx 2T_e^{\text{hot}}[\ln(t_p + \sqrt{t_p^2 + 1})]^2$ . Here,  $t_p \equiv \omega_{\text{pi}} t_{\text{acc}} / \sqrt{2} \exp(1)$  where  $t_{\text{acc}} \approx 1.3\tau$ , and  $\omega_{\text{pi}} = \sqrt{Zm_e/m_i} \omega_p$  is the ion plasma frequency of the protons with mass  $m_i = 1836m_e$  and charge number  $Z = 1$ . For fixed, ultrashort laser pulse duration  $\tau \ll \sqrt{3672 \exp(1) T_e^{\text{hot}} / (1.3a_0)}$  the equation can be approximated by  $\epsilon_{\max} \propto T_e^{\text{hot}} n_e^{\text{hot}}$  and with  $n_e^{\text{hot}} \propto a_0^2 / T_e^{\text{hot}}$  [24] it becomes independent of  $T_e^{\text{hot}}$ ,  $\epsilon_{\max} \propto \tau^2 a_0^2 - O(\tau^4 a_0^4 / T_e^{\text{hot}})$ , proportional to the laser intensity. The linear scaling of maximum ion energy with intensity has been found before by Zeil *et al.* [25] using an alternative ion acceleration model developed in [24] and suggests that by optimizing laser pulse energy and duration high-repetition short-pulse laser systems can be favorable in terms of efficiency of laser-driven ion acceleration if compared to long pulse laser systems.

Our model is chosen to resemble the situation of high-contrast high-intensity laser-matter interaction but ceases to be valid in the case of very long pulse duration or in the presence of intense prepulses or ASE pedestals, since the assumption of predominant laser absorption at the critical density surface interface may become invalid as the laser energy can be reduced in the interaction with the preplasma. Furthermore, we do not take into account the electron temperature increase due to longitudinal and transverse refluxing of electrons, though our findings can be easily adopted in models describing the electron energy enhancement [26].

In contrast to the standard ponderomotive scaling model, the approach presented here focuses on the ensemble dynamics at the critical density interface, taking into account the distribution of electrons with respect to the laser phase. A simple analysis of the interaction dynamics at the critical surface shows that the most energetic electrons detach from the interface when the longitudinal  $v \times B$  force is maximum. With this assumption, validated by PIC simulations, our model can be naturally connected to transport models describing the energy and momentum transfer of these hot electrons into the target bulk and thus lead to a more complete understanding of the energy transfer in laser-matter interactions.

This work was partially supported by the joint research project on COOPTics under Grant No. 03ZIK445. The authors would like to thank the HZDR HPC group for their support.

\*t.kluge@hzdr.de

[1] A. J. Kemp, Y. Sentoku, M. Tabak, *Phys. Rev. Lett.* **101**, 075004 (2008).

- [2] P. Mulser, D. Bauer, and H. Ruhl, *Phys. Rev. Lett.* **101**, 225002 (2008).
- [3] M. G. Haines *et al.*, *Phys. Rev. Lett.* **102**, 045008 (2009).
- [4] P. Gibbon, *Short Pulse Laser Interactions With Matter: An Introduction* (Imperial College Press, London, 2005).
- [5] D. W. Forslund *et al.*, *Phys. Rev. A* **11**, 679 (1975).
- [6] D. F. Price *et al.*, *Phys. Rev. Lett.* **75**, 252 (1995).
- [7] F. Brunel, *Phys. Rev. Lett.* **59**, 52 (1987); *Phys. Fluids* **31**, 2714 (1988).
- [8] S. C. Wilks *et al.*, *Phys. Rev. Lett.* **69**, 1383 (1992).
- [9] B. Bezzerides, S. J. Gitomer, and D. W. Forslund, *Phys. Rev. Lett.* **44**, 651 (1980).
- [10] J. D. Jackson, *Classical Electrodynamics* (John Wiley & Sons, Inc., Hoboken, NJ, 1975), 2nd ed., p. 607.
- [11] R. A. Snavely *et al.*, *Phys. Rev. Lett.* **85**, 2945 (2000).
- [12] T. Kluge *et al.*, *Phys. Plasmas* **17**, 123103 (2010).
- [13] S. C. Wilks *et al.*, *Phys. Plasmas* **8**, 542 (2001).
- [14] M. C. Kaluza, Ph.D. thesis, Technische Universität München, 2004.
- [15] T. C. Pesch and H.-J. Kull, *Phys. Plasmas* **14**, 083103 (2007); C. Max and F. Perkins, *Phys. Rev. Lett.* **27**, 1342 (1971).
- [16] W. L. Kruer and K. Estabrook, *Phys. Fluids* **28**, 430 (1985).
- [17] J. Yu *et al.*, *Phys. Plasmas* **6**, 1318 (1999).
- [18] Hui Chen *et al.*, *Phys. Plasmas* **16**, 020705 (2009).
- [19] F. N. Beg *et al.*, *Phys. Plasmas* **4**, 447 (1997).
- [20] MacPhee *et al.*, *Rev. Sci. Instrum.* **79**, 10F302 (2008).
- [21] Y. Sentoku and A. J. Kemp, *J. Comput. Phys.* **227**, 6846 (2008).
- [22] P. Mora, *Phys. Rev. Lett.* **90**, 185002 (2003).
- [23] J. Fuchs *et al.*, *Nature Phys.* **2**, 48 (2005).
- [24] J. Schreiber *et al.*, *Phys. Rev. Lett.* **97**, 45005 (2006).
- [25] K. Zeil *et al.*, *New J. Phys.* **12**, 045015 (2010).
- [26] T. Kluge, W. Enghardt, S. D. Kraft, U. Schramm, K. Zeil, T. E. Cowan, and M. Bussmann, *Phys. Plasmas* **17**, 123103 (2010); J. Pšikal *et al.*, *Czech. J. Phys.* **56**, B515 (2006); A. J. Mackinnon *et al.*, *Phys. Rev. Lett.* **88**, 215006 (2002); D. Neely *et al.*, *Appl. Phys. Lett.* **89**, 021502 (2006).